2019 12th Asian Control Conference (ASCC)
Kitakyusyu International Conference Center
Japan, June 9-12, 2019

Dynamic Inversion-Based Sliding Mode Control of a Tilt Tri-Rotor UAV

Li Yu, Guang He, Shulong Zhao and Xiangke Wang

Abstract— **The modeling and controller design for a tilt tri-rotor unmanned aerial vehicle (UAV) is studied in this paper. Taking the advantages of high cruise efficiency and vertical takeoff and landing(VTOL) capability, the tilt tri-rotor UAV attracts many researchers' attentions. However, due to the existing nonlinearities and time-varying structure, research on the modeling and control scheme of the tilt tri-rotor UAV is still a challenging work. To achieve stable flight control in helicopter mode, a robust and efficient controller is developed. First, the aircraft is described in detail, and the mathematical model of the aircraft is obtained. Then, a control allocation algorithm is developed to improve modeling precision. Finally, a hierarchical flight controller is designed by combining the theory of dynamic inversion and sliding mode control. The results show that the proposed control scheme can achieve strong robustness.**

I. INTRODUCTION

The tilt-rotor UAV has three flight modes including the helicopter mode, the fixed-wing mode, and the transition mode. Therefore, it enjoys many advantages, such as long endurance, high mobility, and less site limitation. Due to these advantages, tilt-rotor UAV has drawn considerable interest from military and civilian [1].

At present, many countries such as the Uinted states, Korea, Israel and China, etc, are engaged in the development of the tilt-rotor UAV. The United states has made significant achievements by producing V-22 and Eagle Eye. Korea has developed a tilt-rotor UAV named Smart UAV which adapt sliding mode control scheme to satisfy the desired performance under varying loads [2]-[4]. Besides, they also utilize fuzzy control to enable automatic selection of the control laws in the transition mode [5]. In Israel, the Israel Aircraft Industries (IAI) designs a tilt tri-rotor UAV "panther" [6], with maximum take-off weight of 65kg and 4-hour duration. It adapts a Segmented Control Strategy to obtain Steady flight in the transition mode process. Song has designed a flight control law based on the inner/outer loop control structure, and verified an eigenstructure assignment algorithm by the wind tunnel tests [7]. For a flying-wing UAV called TURAC with two tilt rotors and one main coaxial fans, Ugur Ozdemir establishes the mathematical model in different modes. Also, the mode transition strategy is proposed according to the aerodynamic characteristics obtained by CFD [8],[9].

Although many researchers have engaged in the controller design for tilt tri-rotor UAV and lots of useful control methods and views are proposed, there still exist many problems and difficulties to be solved. For one part, control allocation contributes to simplifying the dynamics, nonetheless, few papers pay attention to that. For the other part, the plant is time-varying and nonlinear because of the tilting motion of the motors, which bring enormous challenges in robust controller design for the whole system.

In this paper, we foucus on the robust controller design for the tilt tri-rotor UAV in helicopter mode. First of all, the dynamics model is built by using rotor coefficients obtained through experiments and least square fitting. Then, according to the structure characters of the aircraft, control allocation algorithm is discussed for the tilt tri-rotor UAV. Based on the hierarchical strategy, the proposed controller in this paper is divided into two parts. The SMC control approach is used for outer-loop to reject the unknown external disturbances, In inner-loop, the SMC and the dynamic inversion control approach are combined to improve robustness.

The rest of the paper is organized as follows. Section 2 describes the prototype and mathematical model of the tilt tri-rotor UAV. Also, a novel control allocation algorithm is discussed. The design of the controller and proof of stability are presented in Section 3. The results of simulation and are shown in Section 4. Section 5 gives some conclusion of this paper.

II. MODELING OF TILT TRI-ROTOR UAV

A. Description of Tilt Tri-rotor UAV

The tilt tri-rotor UAV has three flight modes, and these different modes are controlled by different schemes. In the helicopter mode, position control is achieved by the adjustment of attitude. Five actuators including three rotors and two servos are used to control attitude. The right rotor and rear rotor rotate in counterclockwise while the left in clockwise. The two front rotors are able to tilt from 30° to -90°, and the rear rotor is installed vertically. Interference between the rotor and the wing can be neglected due to the distance from the leading edge to the rotor is long enough. The different thrusts between the left and right rotors are used to control the roll motion. The rear rotor can compensate the moment generated by two front rotors to stabilize the pitch. The yaw moment is created by the difference of tilting angles between the two front rotors. The concept of attitude control in the helicopter mode is shown in Fig. 1.

Three-dimensional modeling software CATIA and physical measurements are adopted to acquire the position of different rotors. The coefficients k_f and k_d of the rotor are obtained based on the least square method [10]. The moments of inertia are measured by the oscillation method

The authors are with the College of Mechanics and Automation, National University of Defense Technology, 109 Deya St, Changsha, 410073, China. yulisdu@163.com, heguang410@163.com, jaymaths@nudt.edu.cn, xkwang@nudt.edu.cn

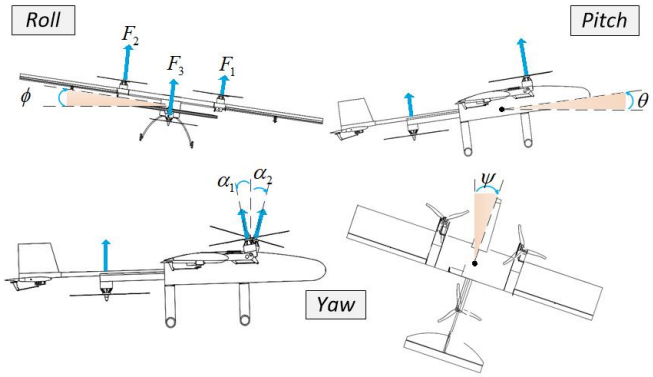

Fig. 1. Attitude Control Principles

[11]. The parameters of the tilt tri-rotor UAV are shown in Table 1.

TABLE I
MODELING PARAMETERS

Symbol	Description	Magnitude
m	mass	5.6 kg
r_{1x}	Right rotor distance along x axis	0.22 m
r_{1y}	Right rotor distance along y axis	0.2635 m
r_{1z}	Right rotor distance along z axis	0 m
r_{3x}	rear rotor distance along x axis	-0.42 m
r_{3y}	rear rotor distance along y axis	0 m
r_{3z}	rear rotor distance along z axis	0 m
k_f	Force coefficient	4.531×10^{-5}
k_d	Torque coefficient	9.409×10^{-7}
I_{xx}	Moment of inertia around x axis	0.3556 $kg \cdot m^2$
I_{yy}	Moment of inertia around y axis	0.3553 $kg \cdot m^2$
I_{zz}	Moment of inertia around z axis	0.6084 $kg \cdot m^2$

The mathematical model of the tilt tri-rotor UAV containing kinematic equations, navigation equations, force equations, and moment equations, is expressed as follows [12]:

$$\begin{cases} \dot{\Theta} = R_{BER} \cdot \omega_b \\ \dot{\chi} = R_{BET} \cdot V \\ \dot{V} = g \cdot \Delta + \dfrac{F^b}{m} - \omega_b \times V \\ \dot{\omega}_b = -I_b^{-1}(\omega_b \times (I_b \cdot \omega_b) - \tau^b) \end{cases} \tag{1}$$

where Δ is defined as

$$\Delta = \begin{bmatrix} -sin\theta \\ sin\phi cos\theta \\ cos\phi cos\theta \end{bmatrix} \tag{2}$$

In these expressions, $\Theta = [\phi, \theta, \psi]^T$ represents the vector of Euler angle, and the position of the center of mass in the world frame is expressed as $\chi = [X, Y, Z]^T$. The rotation matrix from the body frame to the world frame is R_{BER}, and R_{BET} denotes the velocity transformation matrix from the body frame to the world frame.

B. Control allocation

In this part, the design of the control allocation which provides the mapping from the virtual control command to the manipulated inputs is presented [13]. The tilt tri-rotor UAV has four virtual control command $[R, P, Y, T]^T$. R is directly linked to the roll control, P is used for the pitch control, Y is related to the yaw control, and the altitude is controlled by T. The control allocation is used to compute the control inputs $[\omega_1^2, \omega_2^2, \omega_3^2, \alpha_1, \alpha_2]^T$ of five actuators from the virtual control command $[R, P, Y, T]^T$.

The change of rotate speed is faster than the change of tilting angles. According to the response speed of actuators, the calculation of actual outputs is divided into two parts. For the first part, the rotate speeds of the three rotors are acquired by R, P and T. It is noted that the tilting angles are determined when calculating ω_1, ω_2 and ω_3.

$$\begin{bmatrix} R \\ P \\ T \end{bmatrix} = H \begin{bmatrix} \omega_1^2 \\ \omega_2^2 \\ \omega_2^2 \end{bmatrix} \tag{3}$$

where

$$H = \begin{bmatrix} -k_f r_{1y} c\alpha_1 + k_d s\alpha_1 & -k_f r_{2y} c\alpha_2 - k_d s\alpha_2 & 0 \\ k_f r_{1x} c\alpha_1 & k_f r_{2x} c\alpha_2 & k_f r_{3x} \\ k_f c\alpha_1 & k_f c\alpha_2 & k_f \end{bmatrix} \tag{4}$$

where c and s is symbolize cosine and sine functions, respectively. Since the matrix H is a square matrix, the key point to obtain rotate speed $[\omega_1^2, \omega_2^2, \omega_2^2]^T$ is to verify the reversibility of H matrix. Taking the construction symmetry into account, it is clear that we have conditions as

$$\begin{cases} r_{1x} = r_{2x} \\ \alpha_1 = -\alpha_2 \end{cases} \tag{5}$$

In this manner, the determinant of matrix H can be written as

$$|H| = -2k_f^3 r_{1y}(r_{1x} - r_{3x})(cos\alpha_1)^2 \tag{6}$$

Due to the tilting angles are limited $|\alpha_1| \leq \dfrac{\pi}{6}$ in the helicopter mode, then we can conclude that

$$|H| \neq 0 \tag{7}$$

According to the above derivation, the reversibility of H matrix is proved, so that the rotate speeds can be obtained as follows

$$\begin{bmatrix} \omega_1^2 \\ \omega_2^2 \\ \omega_2^2 \end{bmatrix} = H^{-1} \begin{bmatrix} R \\ P \\ T \end{bmatrix} \tag{8}$$

For the second part, there are two tilting angles need to be determined based on Y and $[\omega_1^2, \omega_2^2, \omega_3^2]^T$. The yaw control of the aircraft is achieved by the differential tilting angles generated by two front servos. Two methods can be applied to acquire tilting angles.

(a) Moment balance method:

$$\begin{cases} Y = k_f(\omega_1^2 r_{1y} s\alpha_1 + \omega_2^2 r_{2y} s\alpha_2) \\ \qquad + k_d(\omega_1^2 c\alpha_1 - \omega_2^2 c\alpha_2 + \omega_3^2) \\ \alpha_1 + \alpha_2 = 0 \end{cases} \tag{9}$$

In helicopter mode, a small differential angle between two front rotors can generate enough moment to adjust the yaw

motion. It is reasonable to make an assumption that the tilting angles are small, so that α_1 and α_2 can be obtained as follows

$$\begin{cases} \alpha_1 = \dfrac{Y - k_d(\omega_1^2 - \omega_2^2 + \omega_3^2)}{k_f(\omega_1^2 r_{1y} - \omega_2^2 r_{2y})} \\ \alpha_2 = -\alpha_1 \end{cases} \tag{10}$$

(b) Proportion control method:

$$\begin{cases} \alpha_1 = \delta \cdot Y \\ \alpha_2 = -\delta \cdot Y \end{cases} \tag{11}$$

where δ is a small constant that determined by the maximum tilting angle and the yaw moment. According to the simulation analysis, if the aircraft hover in a point, $\omega_1 \approx 620 rad/s$, $\omega_2 \approx 620 rad/s$ and $\omega_3 \approx 640 rad/s$. We can estimate the yaw moment while the tilting angle $\alpha_1 = 30^\circ$. The value of the yaw moment is obtained as $Y \approx 5.3$, so that the constant δ is given as

$$\delta = \alpha_1 / Y = \frac{30 \cdot 2\pi/360}{5.3} \approx 0.1 \tag{12}$$

Moment balance method is based on the assumption that the tilting angles are small enough and depends on the value of the rotate speeds. Proportion control method is a simple proportional control irrelevant to the rotate speeds, and the kind of decoupling makes it easier to control the yaw motion.

III. CONTROL DESIGN

The control allocation contributes to simplifying the complex dynamics to a single body. In this paper, the control scheme which has a multiloop structure is proposed. The outer-loop is used for position control, and the inner-loop handles the attitude of tilt tri-rotor UAV. The reference command $[X_c, Y_c, Z_c]^T$ is sent to the outer-loop controller and outputs the roll angle ϕ_c, the pitch angle θ_c and the virtual force T for the inner-loop controller. Due to the dynamics of angular rates are faster than the Euler angles, the design of the inner-loop controller is separated into two steps in response to the fast loop and the slow loop. A block diagram of the developed controller architecture is shown in Fig. 2.

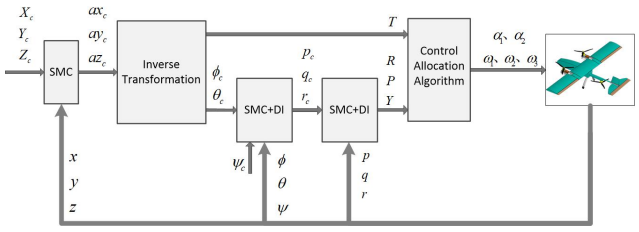

Fig. 2. Block diagram of the flight control system

A. Attitude Controller

This paper presents a two-loop cascade control method. The control performance of the inner-loop is the foundation of the outer-loop. The attitude command $[\phi_c, \theta_c, \psi_c]^T$ is the input of the attitude controller, and the output is the virtual control command $[R, P, Y]^T$. The attitude controller contains fast loop and slow loop. For the first part, the virtual command can be obtained from desired angular rates. First, we rewrite the last equation in (1) mentioned above.

$$\begin{bmatrix} \dot{p} \\ \dot{q} \\ \dot{r} \end{bmatrix} = \begin{bmatrix} c_1 qr \\ c_2 pr \\ c_3 pq \end{bmatrix} + \begin{bmatrix} c_4 & 0 & 0 \\ 0 & c_5 & 0 \\ 0 & 0 & c_6 \end{bmatrix} \begin{bmatrix} \tau_x^b \\ \tau_y^b \\ \tau_z^b \end{bmatrix} \tag{13}$$

where

$$\begin{cases} c_1 = \dfrac{I_y - I_z}{I_x}, & c_4 = \dfrac{1}{I_x} \\ c_2 = \dfrac{I_z - I_x}{I_y}, & c_5 = \dfrac{1}{I_y} \\ c_3 = \dfrac{I_x - I_y}{I_z}, & c_6 = \dfrac{1}{I_z} \end{cases} \tag{14}$$

According to the formulation of dynamic inversion, (13) becomes

$$\begin{bmatrix} R \\ P \\ Y \end{bmatrix} = \begin{bmatrix} c_4 & 0 & 0 \\ 0 & c_5 & 0 \\ 0 & 0 & c_6 \end{bmatrix}^{-1} \left(\begin{bmatrix} v_p \\ v_q \\ v_r \end{bmatrix} - \begin{bmatrix} c_1 qr \\ c_2 pr \\ c_3 pq \end{bmatrix} \right) \tag{15}$$

The control input $[v_p, v_q, v_r]^T$ is designed based on SMC, and the sliding manifolds are designed with an integral term as follows

$$\begin{cases} S_p = c_p \int e_p + e_p \\ S_q = c_q \int e_q + e_q \\ S_r = c_r \int e_r + e_r \end{cases} \tag{16}$$

where $e_p = p_c - p$, and c_p is a constant. To simplify the description, taking the channel of the roll control for example. The exponential approach law is defined to alleviate the chattering problem [14]

$$\dot{S}_p = -\varepsilon_p sat S_p - k_p S_p, \quad \varepsilon_p > 0, k_p > 0 \tag{17}$$

where ε_p and k_p are the positive constants that related to the approaching velocity, and *sat* denotes the saturation function. By (16) and (17), we have

$$\begin{cases} v_p = c_p(p_c - p) + \dot{p}_c + \varepsilon_p sat S_p + k_p S_p \\ v_q = c_q(q_c - q) + \dot{q}_c + \varepsilon_q sat S_q + k_q S_q \\ v_r = c_r(r_c - r) + \dot{r}_c + \varepsilon_r sat S_r + k_r S_r \end{cases} \tag{18}$$

For the second part, the purpose of the slow loop is to derive desired angular rate $[p_c, q_c, r_c]^T$ for the fast loop from the command $[\phi_c, \theta_c, \psi_c]^T$. The first equation in (1) can be expanded as

$$\begin{bmatrix} \dot{\phi} \\ \dot{\theta} \\ \dot{\psi} \end{bmatrix} = \begin{bmatrix} 1 & sin\phi tan\theta & cos\phi tan\theta \\ 0 & cos\phi & -sin\phi \\ 0 & sin\phi sec\theta & cos\phi sec\theta \end{bmatrix} \begin{bmatrix} p \\ q \\ r \end{bmatrix} \tag{19}$$

If pitch angle $\theta \neq \pm\dfrac{\pi}{2}$, we have

$$\begin{bmatrix} p_c \\ q_c \\ r_c \end{bmatrix} = \begin{bmatrix} 1 & sin\phi tan\theta & cos\phi tan\theta \\ 0 & cos\phi & -sin\phi \\ 0 & sin\phi sec\theta & cos\phi sec\theta \end{bmatrix}^{-1} \begin{bmatrix} v_\phi \\ v_\theta \\ v_\psi \end{bmatrix} \tag{20}$$

SMC is used to yield control input

$$S_\phi = c_\phi \int e_\phi + e_\phi \tag{21}$$

where $e_\phi = \phi_c - \phi$, and c_ϕ is a constant.

$$\dot{S}_\phi = -\varepsilon_\phi sat S_\phi - k_\phi S_\phi, \;\; \varepsilon_\phi > 0, k_\phi > 0 \tag{22}$$

By (21) and (22), we can derive control input for (20)

$$\begin{cases} v_\phi = c_\phi(\phi_c - \phi) + \dot{\phi}_c + \varepsilon_\phi sat S_\phi + k_\phi S_\phi \\ v_\theta = c_\theta(\theta_c - \theta) + \dot{\theta}_c + \varepsilon_\theta sat S_\theta + k_\theta S_\theta \\ v_\psi = c_\psi(\psi_c - \psi) + \dot{\psi}_c + \varepsilon_\psi sat S_\psi + k_\psi S_\psi \end{cases} \tag{23}$$

The control law of the fast and slow loop are designed based on exponential approach law. In order to analyze the stability of the attitude controller, a global Lyapunov function candidate is defined as

$$\sigma = \frac{1}{2} S^2 \tag{24}$$

The time derivative of the Lyapunov function is

$$\dot{\sigma} = S\dot{S} = -\varepsilon |S| - kS^2 \tag{25}$$

By substituting (24) into (25)

$$\dot{\sigma} = -\varepsilon |S| - 2k\sigma \tag{26}$$

Considering the constraint of ε, (26) can be rewritten as

$$\dot{\sigma} < -2k\sigma \tag{27}$$

We select $\eta = \dot{\sigma} + 2k\sigma$, it is obviously that $\eta < 0$, so that we can obtain

$$\dot{\sigma} = -2k\sigma + \eta \tag{28}$$

Basing on the theory of variable upper limit integral, from (28), the integration is calculated as

$$\begin{aligned} \sigma(t) &= e^{-2k(t-t_0)}\sigma(t_0) + \int_{t_0}^{t} e^{-2k(t-\iota)}\eta(\iota)d\iota \\ &< e^{-2k(t-t_0)}\sigma(t_0) \end{aligned} \tag{29}$$

Therefore, the controller allows the states converge to the desired point in finite time.

B. Position Controller

Position control is realized by the change of attitude, and the desired roll angle ϕ_c and pitch angle θ_c are references for the attitude subsystem. The aim of the position controller is to compute control inputs T, ϕ_c and θ_c. The design of the position controller is divided into two steps. The first step is to build the relationship between the virtual accelerations and the control inputs.

$$\begin{bmatrix} T_X \\ T_Y \\ T_Z \end{bmatrix} = R_{BET} \begin{bmatrix} 0 \\ 0 \\ -T \end{bmatrix} \tag{30}$$

It can be equivalently expressed as

$$\begin{cases} T_X = -(c\phi s\theta c\psi + s\phi s\psi)T \\ T_Y = -(c\phi s\theta s\psi - s\phi c\psi)T \\ T_Z = -(c\phi c\theta)T \end{cases} \tag{31}$$

The relationship between the forces and the accelerations is defined as

$$\begin{cases} T_X = ma_X \\ T_Y = ma_Y \\ T_Z = m(a_Z + g) \end{cases} \tag{32}$$

From (31) and (32), if the desired yaw angle ψ_c is determined, then, we have

$$\begin{cases} T = m\sqrt{a_X^2 + a_Y^2 + (a_Z + g)^2} \\ \phi_c = \arcsin\left(m\left(a_Y c\psi_c - a_X s\psi_c\right)/T\right) \\ \theta_c = \arcsin\left(\left(-ma_X - Ts\phi_c s\psi_c\right)/\left(Tc\phi_c c\psi_c\right)\right) \end{cases} \tag{33}$$

For the second step, SMC is utilized to compute these virtual accelerations, and the sliding manifold is given as

$$S_X = c_X e_X + \dot{e}_X \tag{34}$$

where $e_X = X_c - X$, the exponential approach law is applied, and we have

$$\begin{cases} a_X = c_X\left(\dot{X}_c - \dot{X}\right) + \ddot{X}_c + \varepsilon_X sat S_X + k_X S_X \\ a_Y = c_Y\left(\dot{Y}_c - \dot{Y}\right) + \ddot{Y}_c + \varepsilon_Y sat S_Y + k_Y S_Y \\ a_Z = c_Z\left(\dot{Z}_c - \dot{Z}\right) + \ddot{Z}_c + \varepsilon_Z sat S_Z + k_Z S_Z \end{cases} \tag{35}$$

Note that the desired yaw angle can be set to any reference value. The desired roll angle, pitch angle and virtual force can be obtained by the two steps above.

IV. SIMULATION AND DISCUSSION

The performance of the proposed control scheme is investigated via numerical simulations carried out in the Simulink environment. In this section, the control system is examined for its ability to reject low-frequency disturbances, and the robustness against system parameter perturbation is also tested. For the tracking capability test, a complete flight scenario simulation is carried out. Note that the Z axis in the world frame is directed downwards, but for display purpose, the value of altitude is transformed into positive in this part.

A. Performance Analysis

In this part, the control system is assessed in terms of robustness and capabilities. On one hand, the controller is examined for its ability to reject the low-frequency disturbance. On the other hand, it is tested for its robustness against model parameter variation. It is assumed that the aircraft has been tested by the step input and hovering at a fixed point before a low-frequency sinusoidal disturbance is applied to the Z axis. To verify the capability of rejecting disturbance, the system performance is verified through introducing an external disturbance input

$$d(t) = \begin{cases} 0.5sin(0.5\pi(t-6)), & 6 \le t \le 10 \\ 0, & t < 6, t > 10 \end{cases} \tag{36}$$

The external disturbance is added into the system in $6s - 10s$. The step test results are shown in Fig. 3.

It is observed that the tilt tri-rotor UAV is able to track the desired position in 3 seconds. Although the external disturbance is applied, the altitude of the aircraft is almost

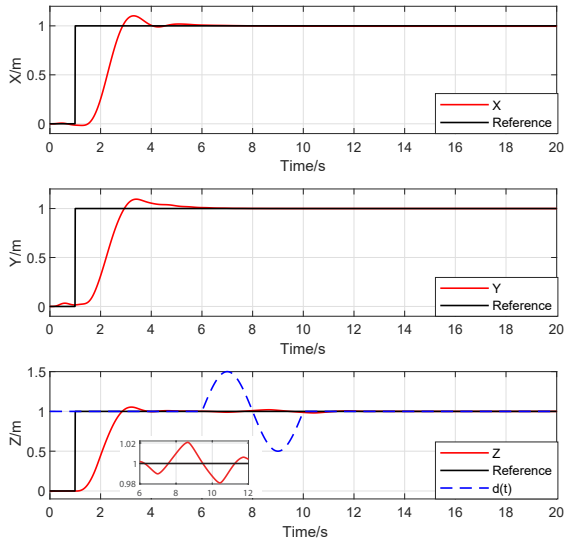

Fig. 3. Step response of position

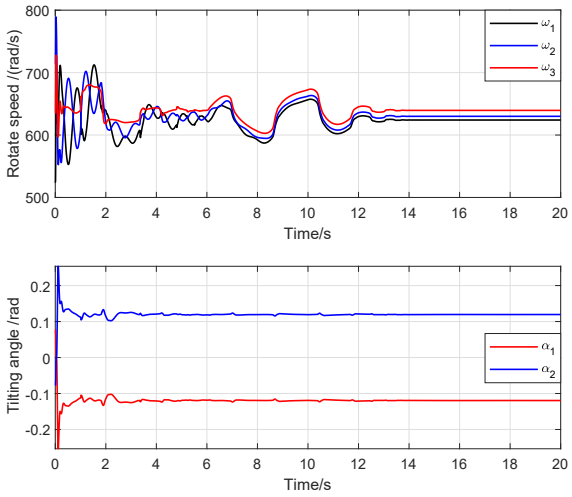

Fig. 4. Actual outputs

unchanged. Fig. 4 shows that the outputs are constrained without saturation. This advantage contributes to reducing the flight risk. The simulation results show that this control system has good stability and strong anti-interfering power.

In order to verify the robustness of the control system, several model parameters are changed as shown in Table 2. The same step test is applied to the control system with uncertainties.

Under the influence of the uncertainties, the response time of the control system is longer than the normal situation but still has a satisfactory control effect. Simulation results show that the proposed control scheme exhibits strong robustness.

B. Flight Simulation Results

To demonstrate the performance of the control system in the helicopter mode, the desired trajectory for tilt tri-rotor UAV is generated in terms of position vector $[X,Y,Z]^T$. The desired and actual trajectories for the tilt tri-rotor UAV are

TABLE II
VARIATION OF MODEL PARAMETERS

Symbol	Variation	Symbol	Variation
m	120%	I_{xx}	120%
k_f	80%	I_{yy}	120%
k_d	120%	I_{zz}	120%

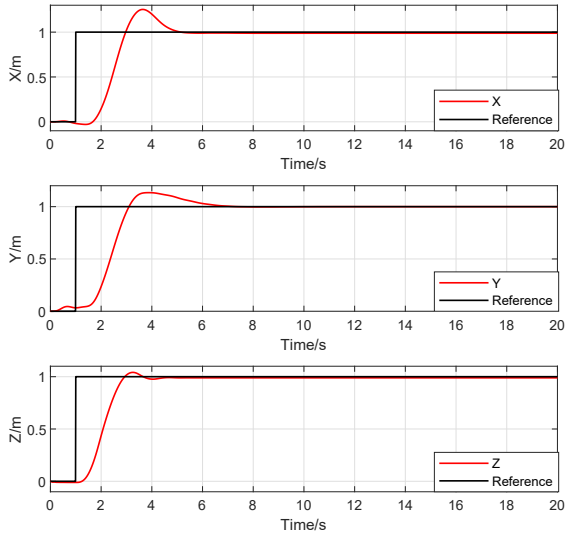

Fig. 5. Model parameters uncertainty test results

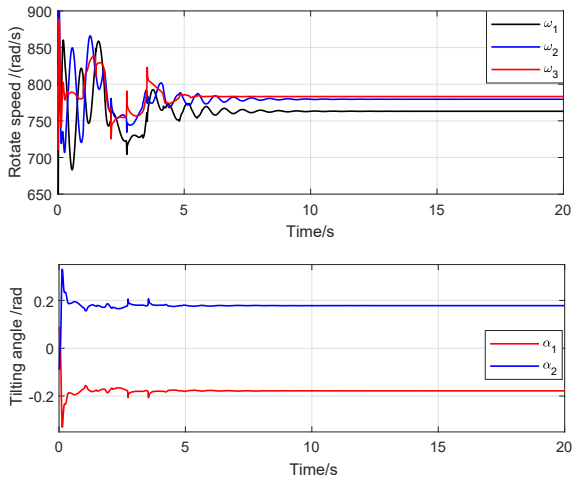

Fig. 6. Actual outputs

shown in Fig. 7. It is noticed that the whole simulation is completed within 60 seconds, and the horizontal flight takes place from the $10th$ to the $50th$ second. The Euclidean position error is shown in Fig. 8. As can be seen in these figures, the sliding mode controller provides satisfactory position tracking with the maximum position error less than $0.32m$. The responses for the Euler angles are given in Fig. 9, and it shows that the inner-loop controller yields effective command following for the given references.

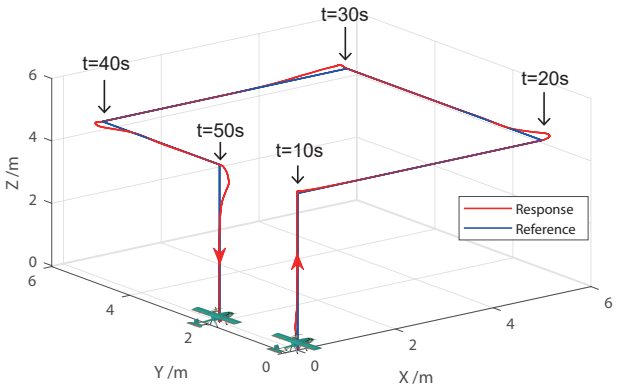

Fig. 7. Reference trajectory and actual position of the aircraft

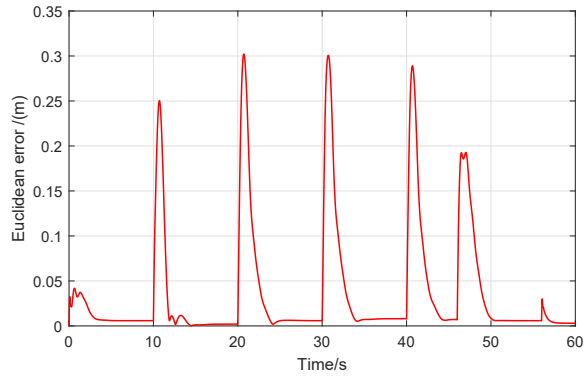

Fig. 8. Euclidean position error

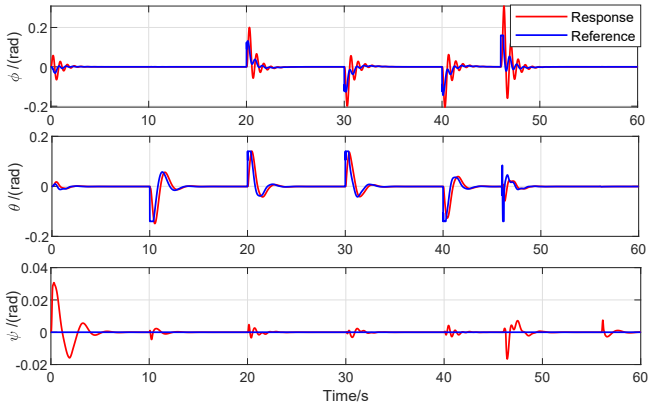

Fig. 9. Euler angles

V. CONCLUSIONS

The tilt tri-rotor UAV is a novel aircraft with special configuration, and the stable flight control in the helicopter mode is the foundation of mode switching. In this article, the sliding mode control strategy based on dynamic inversion is proposed to achieve stable flight control. Firstly, to improve the accuracy of the model, several significant parameters are obtained. Then, a control allocation algorithm is developed to simplify the complex model to a single body system with forces and moments as control inputs. A control scheme with a multiloop structure is proposed, so that the position and attitude controllers can be constructed independently. Thanks to the robustness of the proposed control scheme, uncertainties in the model can be handled without the need for parameter estimation. Finally, simulation results show that the control scheme provides satisfactory tracking for the given position references with acceptable errors.

The next step in this research will focus on the attitude control of tilt tri-rotor UAV in the transition mode. Attitude is controlled by rotor and control surfaces in the special mode, so that an advanced control allocation algorithm is the key to achieving stable mode switching.

REFERENCES

[1] Liu Z, He Y, Yang L, and Han J, "Control techniques of tilt rotor unmanned aerial vehicle systems: A review," *Chinese Journal of Aeronautics*, vol. 30, no. 1, pp. 135-148, 2017.

[2] Lee, Jinoh, et al, "An experimental study on time delay control of actuation system of tilt rotor unmanned aerial vehicle," *Mechatronics*, vol. 22, no. 2, pp. 184-194, 2012.

[3] Kang Y, Park B, Yoo C, and Koo S, "Control law modification according to flight test of small scaled tilt rotor uav," in: *AIAA Guidance, Navigation and Control Conference and Exhibit*, 18-21 August 2008, Honolulu, Hawaii.

[4] Kang Y, Kim N, Kim B S, and Tahk M J, "Autonomous waypoint guidance for tilt-rotor unmanned aerial vehicle that has nacelle-fixed auxiliary wings," in: *Proceedings of the Institution of Mechanical Engineers, Part G: Journal of Aerospace Engineering*, vol. 228, no. 14, pp. 2695-2717, 2014.

[5] Yoo, Chang-Sun, et al, "Actuator controller based on fuzzy sliding mode control of tilt rotor unmanned aerial vehicle," *International Journal of Control, Automation and Systems*, vol. 12, no. 6, pp. 1257-1265, 2014.

[6] Israel Aerospace Industries, http://www.iai.co.il/2013/36944-en/BusinessAreas_UnmannedAirSystems.aspx. Accessed on: March 13, 2018.

[7] SongYanguo and WangHuanjin, "Design of Flight Control System for a Small Unmanned Tilt Rotor Aircraft," *Chinese Journal of Aeronautics*, vol. 22, no. 3, pp. 250-256, 2009.

[8] Ozdemir, Ugur, et al, "Design of a commercial hybrid VTOL UAV system," *Journal of Intelligent and Robotic Systems*, vol. 74, no. 1-2, pp. 371-393, 2014.

[9] Yuksek, Burak, et al, "Transition flight modeling of a fixed-wing vtol uav," *Journal of Intelligent and Robotic Systems*, vol. 84, no. 1-4, pp. 83-105, 2016.

[10] Yu L , Zhang D , Zhang J , et al, "Modeling and attitude control of a tilt tri-rotor UAV," in: *Control Conference. IEEE*, 2017.

[11] Soule, Hartley A, and M. P. Miller, "The experimental determination of the moments of inertia of airplanes," *Technical Report Archive and Image Library* 1934.

[12] V. Klein, E. Morelli, Aircraft System Identification Theory and Practice. Reston, Va, USA: American Institute of Aeronautics and Astronautics, 2006, pp. 33-40.

[13] Seo, Yongjun, and Y. Kim, "Modeling and Attitude Control of Tri-Tilt Ducted Fan Vehicle," in: *AIAA Guidance, Navigation, and Control Conference*, 2015.

[14] Gao. W, and J. C. Hung, "Variable structure control of nonlinear systems: A new approach," *IEEE transactions on Industrial Electronics*, vol. 40, no. 1, pp. 45-55, 1993.